Model Correlation for Mars Pathfinder Entry, Descent and Landing Simulation

Chia-Yen Peng*, Sai K. Tsang*, Kenneth Smith+, Dara Sabahi*, Kendra Short*, Ann Mauritz*

*Jet Propulsion Laboratory
Pasadena, CA 91109, USA

+Structural Dynamics Research Corporation
San Diego, CA 92130, USA

Abstract Two multi-body drop tests were conducted to provide data to calibrate and verify a multi-body dynamics computer model, which was the major analytical tool used to study the entry, descent and landing (EDL) of the Mars Pathfinder mission. A general summary of the tests and important features of the simulation model are presented in this paper. Good correlation between test results and analytical predictions were achieved. This confirmed the validity and accuracy of the model used for a subsequent extensive Monte Carlo effort to study the dynamics of the EDL under various spacecraft configurations and Martian environmental conditions.

TABLE OF CONTENTS

1. INTRODUCTION

Mars Pathfinder is a $150 million unmanned Mars exploration mission designed by the Jet Propulsion Laboratory to deliver a lander, camera and instrument-laden rover to the Martian surface on July 4, 1997. The spacecraft is scheduled to launch from Cape Canaveral in December 1996.

EDL Soft Landing Approach

To meet the mission requirements [1], a sophisticated and unconventional atmospheric entry, descent and landing approach has been developed. As animated in Figure 1, after the spacecraft enters the Mars atmosphere, a parachute will be deployed to slow descent, and the heatshield will be jettisoned when it is no longer needed. As the rest of the spacecraft parachutes down, the lander will be lowered by a 20-meter bridle from the backshell and the rocket's braking system will engage. The bridle will then be cut, releasing the lander surrounded with inflated airbags for a soft landing on the Martian surface.

EDL Dynamic Simulation

In order to prove the EDL concept and to predict the system performance, an end-to-end multi-body dynamic simulation of the entire EDL sequence, Figure 1, has been performed using the ADAMS program [2,3]

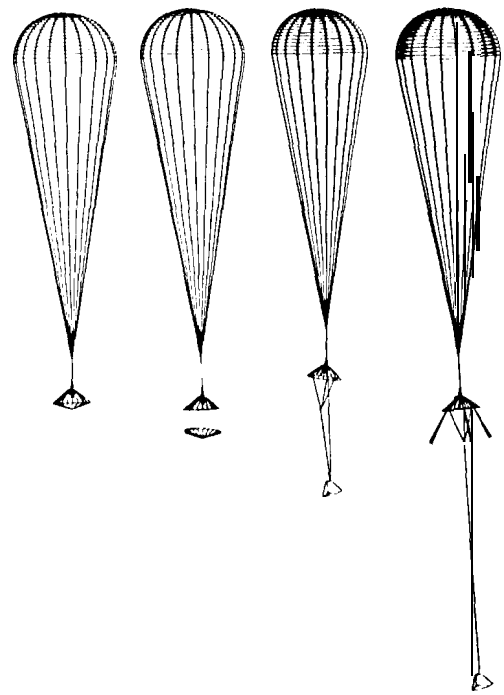

Figure 1. EDL Dynamic Simulation

Since the Mars Pathfinder 1 EDL simulation is essential to the mission success, the dynamic model used in the simulation was verified by model correlation using the data from two multi-body system drop tests:

- EDL System Drop Test;
- Lander Separation Drop Test.

2. EDL SYSTEM DROP TEST

The EDL system drop test was performed over a two week period, from September 28 through October 12, 1995, in Boise, Idaho.

The objective was to provide experimental data to verify the dynamic model of the Mars Pathfinder EDL system in its terminal descent configuration,

Test Configuration

The test article consisted of a parachute, backshell and lander, Figure 2a. The parachute was constructed in flight configuration with a fabric having a permeability coefficient scaled to the Martian atmosphere. As required by the test instrumentation, the parachute canister had non-flight dimensions. The backshell and lander were in full-scale dimensions to simulate their flight aerodynamics. The mass of the backshell and lander was bad on the 3/8th scaled Mars mass. The 20-meter long lander bridle was the same as flight. The lander bridle Descent Rate Limiter (DRL) was a development test unit assembled by JPL.

Test Measurement

To provide useful data for the subsequent model correlation, the following system response was measured:

- Angular positions (x,y) of backshell and lander;
- Angular rates (z) of backshell and lander;
- Accelerations (x,y,z) of backshell and lander;
- Downward dynamic pressure on lander;

In addition, videos were taken from ground and backshell.

Post Processing of Test Data

Since only the system response under 10 Hz was of interest and the fact that the test data was sampled at a very high rate of 1 KHz, the test data was reduced and processed in four steps:

- Applied a low-pass filter (0-10 Hz) to the raw data;
- Removed the pre- and post-events, and then sampled the actual event at a rate of 20 Hz. (This reduced the quantity of data by 99%.);
- Applied a Hanning window to the filtered narrow-band data;
- Performed spectral analyses on the windowed data using the Fast Fourier Transform (FFT) technique.

During the data reduction, it was observed that all the angular data were unusable due to the gyros being severely damaged by ground impact. As a result, the angular information had to be recovered from the video recording.

Note that there were two video cameras mounted on the backshell. One recorded an upward view from the backshell to the parachute; the other a downward view from the backshell to the lander. By digitizing, the videos, two view angles were obtained, one up-looking and one down-looking.

Test Analytical Model

As shown in Figures 2b and 2c, a three dimensional multi-body dynamic model of the test configuration was developed for the model correlation. This test analytical model, or TAM, consisted of a disk gap-band parachute, backshell, bridle and lander. The TAM was a modified version of the dynamic model used in the Mars Pathfinder EDL simulation [2].

Analysis Modal Properties

The analysis modal properties (natural frequencies, damping and mode shapes) were predicted by linearizing the TAM in two test configurations [4]: (1) two-body configuration

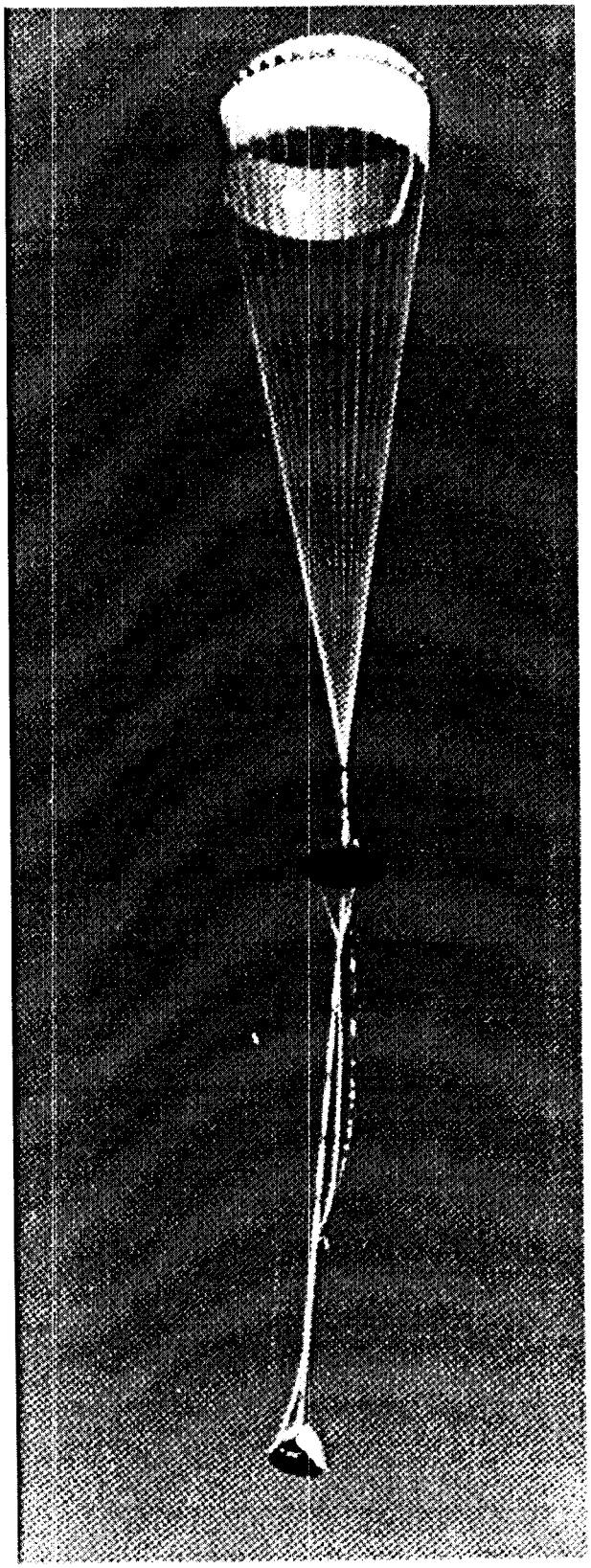

Figure 2a. EDL System Drop Test

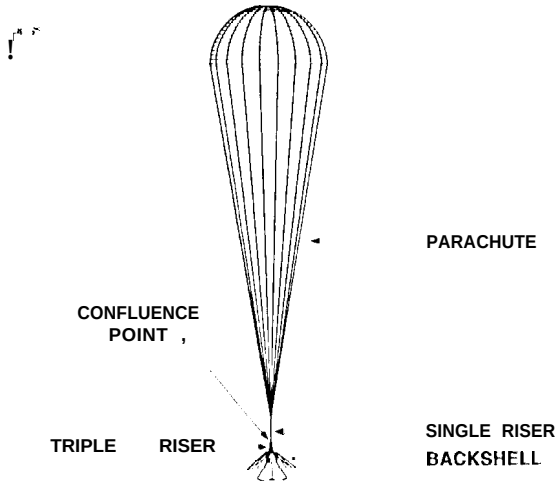

Figure 2b. TAM of EDL System Drop Test (Before Lander Separation)

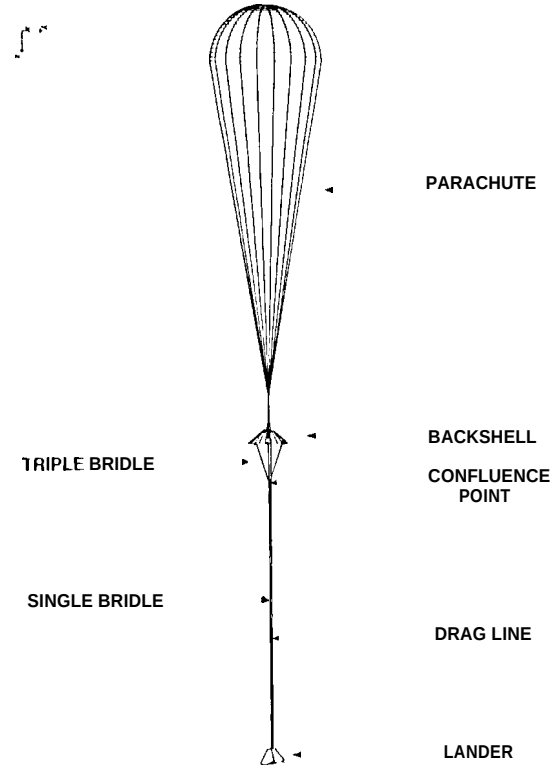

Figure 2c. TAM of EDL System Drop Test (After Lander Separation)

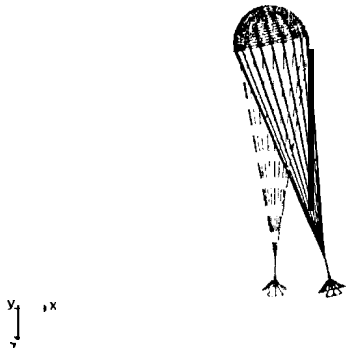

Figure 3a. Two-Body Pendulum Mode
(Before Lander Separation)

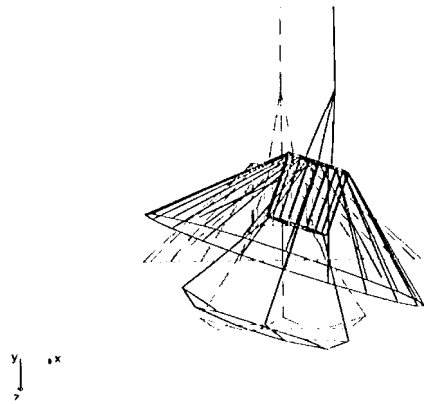

Figure 3b. Entry Body Rotational Mode
(Before Lander Separation)

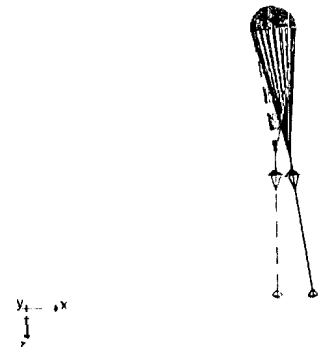

Figure 3c. Three-Body Pendulum Mode
(After Lander Separation)

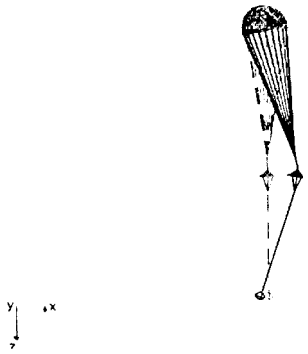

Figure 3d. Three-Body Elbow Mode
(After Lander Separation)

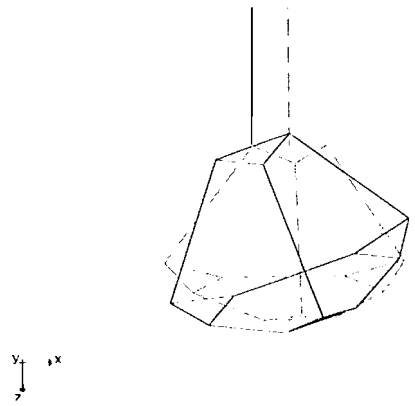

Figure 3e. Lander Wrist Mode
(After Lander Separation)

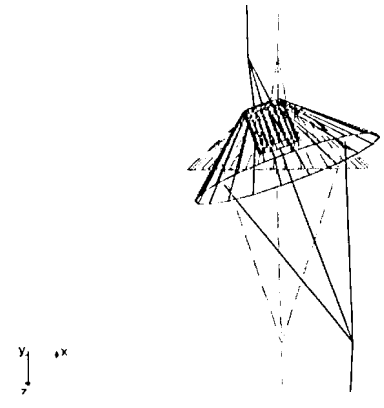

Figure 3f. Backshell Rotational Mode
(After Lander Separation)

before the lander separation, Figure 2b; (2) three-bocly configuration after the lander separation, Figure 2c.

The mode shapes predicted by the TAM are shown in Figures 3a to 3f. Due to symmetry, the system modes are in pairs and only one of each pair is shown. The other is similar in shape, but orthogonal.

Test Modal Properties

FFT spectra of the acceleration data were used to extract the test modal properties, mainly the natural frequencies and damping. The mode shapes were estimated from the videos. A typical acceleration time history and the corresponding FFT spectrum are illustrated in Figure 4.

Note that the FFT spectra of different time segments were examined to identify the system modal properties for the two test configurations mentioned above: (1) 15-20 scc time segment was used for the two-body configuration; (2) 40-1 1 O scc time segment was used for the three-bd *y* configurat i on. The test modal properties are listed in '1'able 1.

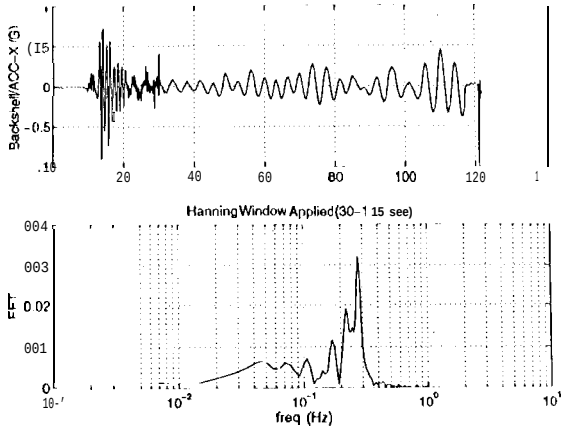

Figure 4. Typical Accel. and FFT Spectrum

3. Moron, CORRELATION FOR ESD TEST

Moss Properties Update

'1 'hc first step of the model correlation process was to thoroughly review and update the mass propert its. The mass properties of each modeled bod y in the '1 'AM were updated based upon either the actual measured weight or the estimates from the CAD model.

Since the frequencies of the local lander and backshell modes are sensitive to their own e.g. z-coordinates. The z-coordinate of the lander e.g. was refined by matching the frequency of the lander wrist mode, Figure 3e. After the adjustment of the lander e.g., the backshell e.g. z-coordinate was updated by correlating the frequency of the entry body rotational mode, Figure 3b.

Damping Coefficients Adjustment

To reflect the high damping observed from the test data, the clamping of the lander wrist mode in the TAM was increased to 5% by adding a rotational damper.

Similar to section 4, the 1)RI, drag coefficient was adjusted from the prc-test value of ().()()55 to 0.0073 based on the lander deployment t ime measured from the data. This shows that the 1)RI, introduced more damping during the test than that predicted by the prc-test 'I AM. As a result, there was very little lander oscillation observed at the end of the lander deployment.

It was also observed that the actual bridle damping was higher than that assumed in the prc-test TAM. Based on the amplitude of snatch acceleration at the end of lander deployment, the bridle damping was increased to 10,000 kg/see.

A erodynamic Model Correlation

'1 he critical parameter for parachute stability is the aerodynamic coefficient of C_N vs. angle of attack which determines the normal component of aerodynamic force acting on the parachute.

The primary 1)DI, system drop t c s t data available for veri fying the parachute C_N arc the up-looking and down-looking view angles. Since the view angles were strongly dependent on the backshell aerodynamic stability, the parachute aerodynamic coefficient C_N was correlated after the backshell wind t u n n e l testing.

In this study, the parachute C_N was parametrized as: $C_N(\alpha) = C_1\sin(\alpha) + C_2\sin^2(\alpha)$, where α is the angle of attack, and C_1 and C_2 are two constant coefficients. With the backshell aerodynamic properties known from wind tunnel test, a total of 336 EDL simulation nms were made with possible ranges of C_1 and C_2. The results are plotted in Figures 5a and 5b.

It was observed that the up-looking view angle varied between 2 to 6 degrees, and the down-looking view angle between 1 to 2.S degrees. To reproduce the view angle ranges observed, the combinations of C_1 and C_2 had to be selected between the contour lines of *2* and 6 degrees (Figure 5a) and those of 1 and 2.5 degrees (Figure 5b). The selected (C_1,C_2) set was used to define the correlated parachute aerodynamic model for the final Mars Pathfinder EDL simulation.

TAM Predictions vs. Test Results

The results are summarized in 'l'able 1 by comparing the modal properties predicted by the correlated TAM and those identified from the test data.

In general very good agreement between the analysis and test modal properties, especially the frequency correlation, was achieved.

4. LANDER SEPARATION DROP TEST

Two lander separation drop (LSD) tests were performed at the Missile 1 ngagement Simulation Arena of China Lake Naval Weapons Center, (California in September and October, 1995.

The objectives were to verify that the mechanical devices for the lander separation would function in their flight configuration as well as to provide test data to validate the model used in the Mars Pathfinder EDL simulation. Confidence in the accuracy of this software was considered to be critical since it was to be used for a subsequent Monte Carlo analysis to study the dynamics of the prototype spacecraft under various Martian conditions.

'1'able 1. ESD Te 'Model Cor lation Results

Description of Mode Shapes	Freq. (Hz)	Damping (%)	Freq. (Hz)	Damping (%)
2-Body Pendulum Modes (Before Lander Separation)	01019 0.1019	14.5 145	n/a (rec. tooshort	n/a (rec. too short)
Entry Body Rotational Modes (Before Lander Separation)	08951 0.9118	5.5 5,5	0.9075 0.9288	- 7 - 7
3Body Pendulun , Modes (After Lander Separation)	00788 0.0789	124 11.8	o 0779 o 0780	- 10 - 10
3-Body Elbow Modes (After Lander Separation)	0.2354 0.2355	0.01 0.23	o 2769 o 2694	-1 - 1
Lander Wrist Modes (After Lander Separation)	0.9891 1.0113	5.2 5.3	o 9429 O 9502	- 4 . 4
Backshell Rotational Modes (After Lander Separation)	1.8847 19711	2 0 2 0	n/a damped)	n/a damped)

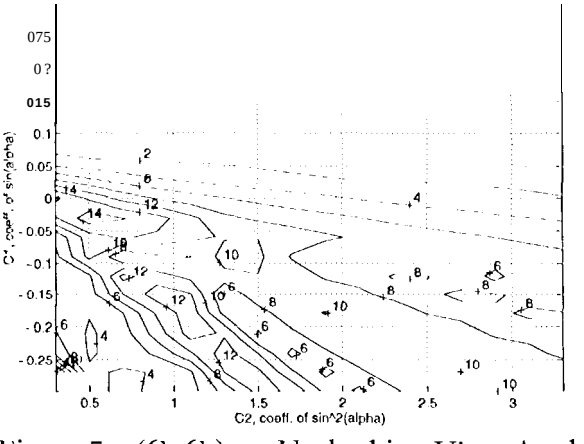

Figure 5a. (C_1,C_2) vs. Up-looking View Angle

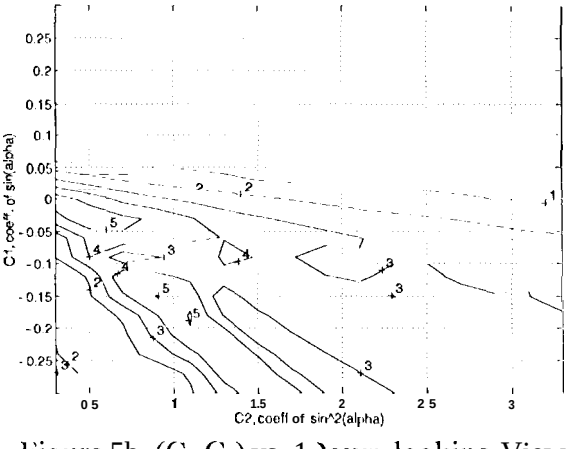

Figure 5b. (C_1,C_2) vs. 1 Down-looking View Angle

Test Configuration

These tests were conducted at ambient temperatures and pressures in an indoor environment to obviate potential complexities caused by wind effects.

The set-up is shown in Figure 6. Prior to separation the lander was attached to the Backshell Interface l'late (1111') with six separation nuts. A drag line was employed to reduce the snatch force on the lander at the end of deployment. This drag line was stored inside a Descent Rate 1 .imiter (DRL) in the form of a payout reel located inside the lander and connected to a point on the backshell at the other end. The lander was also connected to three points on the backshell by a bridle system comprising a single bridle and a triple bridle.

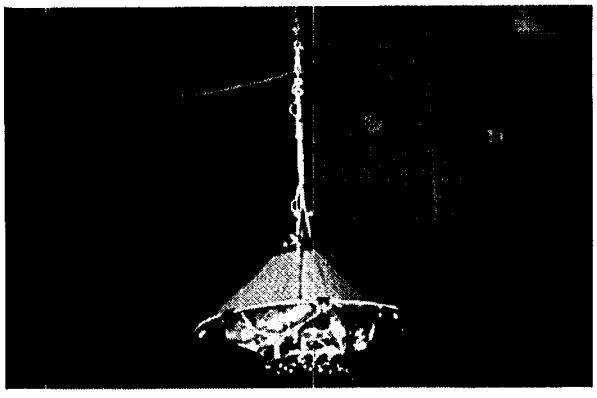

Figure 6. Lander Separation Drop Test Set-uJJ

The lander/backshell assembly was attached to a crane hook with three flexible parachute-]ikc bridles. The crane hook was suspended on a single cable to the ceiling of the build ing,.

The stages of deployment is described in Figure 7.

Twotests were conducted. in LSD Test 1, the backshell/lander assembly was initially suspend ed vertical] y so that prior to separation, all initial velocities were zero. In LSD Test 2, the backshell/lander assembly was pulled with a cable so that it was suspended slightly off vertical. This cable was then cut to enable the backshell/lander assembly to swing in a pendulum motion and separat ion was initiated whi le the assembl y was swinging.

Test Measurement

A string potentiometer, load cells, gyros and accelerometers were used to measure the following system response during the tests:

. Separation distance
. Bridle and reaction forces
. Translation/rotational motions and accelerations of the backshell and lander.

Test A nalytical Models

'1'13c analysis was performed using a mechanical systems simulation software Al)AMS on a HP 735 workstation. The test analytical models were based on the full multi-body model described in section 1.

An analytical animation of the separation event is shown in Figure 8 where the coordinate system is also defined.

The modifications made for the TAM of LSD 'lest 1 are discussed below.

1. Mass properties were adjusted to match measured values. Updated mass values for backshell and lander were 104.31 kg and 175.61 kg respectively.

2. All aerodynamic forces were removed since testing was conducted indoors.

3. Ground boundary condition was imposed above the backshell at the ceiling of the building.

4. Based on measured deployment time, drag coefficient of DRL was adjusted to a value of 0.008. This number when multiplied by the relative velocity of the two end markers was proportional to the drag force.

5. Based on the amplitude of vertical oscillation at the end of deployment, the bridle damping was adjusted to a value of 8000 kg/see. The damping force was

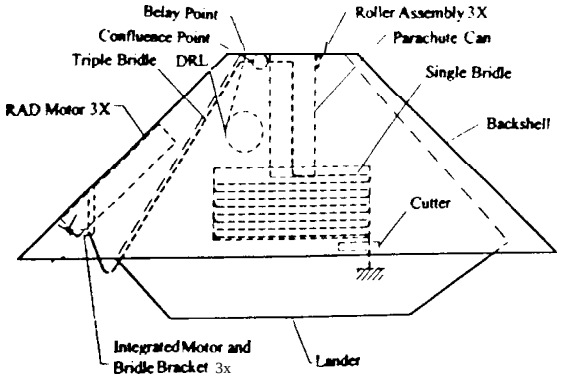

Step 1

- Lander stowed in backshell
- 2 cable cutters fired
- 3 sep nuts fired
- 3 sep nuts fired

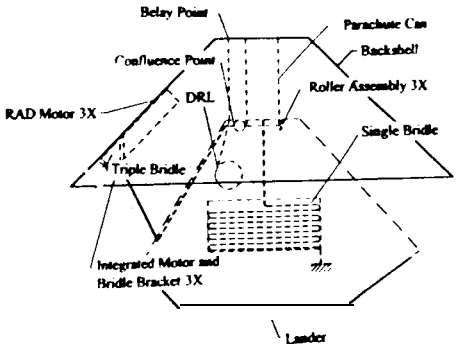

Step 2

- Lander begins to translate along parchute can
- Line begins to payout of descent device
- Triple bridle peels off lander

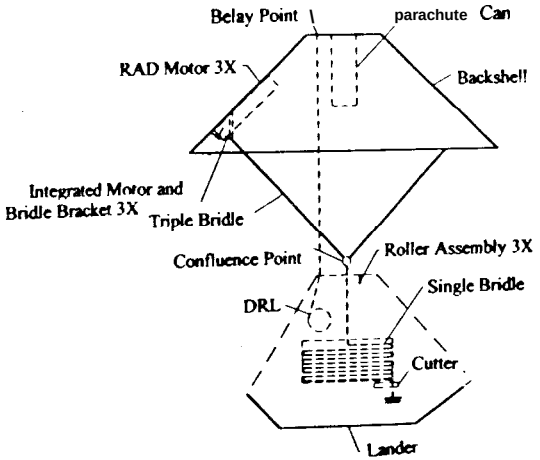

Step 3

- Lander clears backshell
- Triple bridle peels off lander to the confluence point
- Single bridle begins to deploy from anchor box

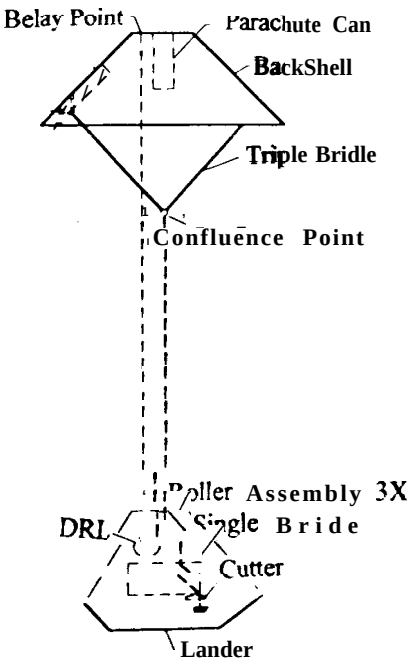

Step 4

- Single bridle continues to deploy
- Lander weight carried by bridle
- Excess descent line still attached to device
- Deployment complete

Figure 7 Deployment Sequence of Backshell/Lander Assembly

obtained by multiplying this number by the relative velocity of the two end markers.

6. Value of acceleration due to gravity changed to 9.806 m/sec^2 to reflect 1 Earth condition

The TAM of LSD Test 2 is identical to the model for LSD Test 1 except:

1. A side force was applied to the backshell to produce the initial pendulum motion. The magnitude of this force was adjusted to match the test data.

2. Based on measured deployment time, drag coefficient of DRL was adjusted to a value of 0.009.

5. MODEL CORRELATION FOR LSD TEST

Important analytical and test results are selected for comparison in this section. The they will be discussed separately for the two tests.

Correlation for LSD Test 1

Figures 9 and 10 show respectively the vertical displacement of the lander c.g. vs. time from test and TAM. The excellent agreement in deployment time was obtained by adjusting the analytical value of the drag coefficient Of the DRL.

The backshell rotation about the Y axis from test and TAM is shown in Figures 11 and 12 respectively. The corresponding relations about the X axis is shown in Figures 13 and 14.

Very good frequency correlation is obtained for both axes for the duration of the lander deployment (t ≈ 2-12 sec). For rotation about the Y axis, the predicted oscillation amplitudes are generally somewhat lower than those obtained from the test while for rotation about the X axis, the amplitude correlation is initially quite good even though the test data indicated higher damping during the later stages of deployment.

Figures 15 and 16 show respectively the lander rotation about the X axis from test and TAM. The difference in frequency between analysis and test result is approximately 8%. Excellent agreement is obtained for the amplitude of the first oscillation. However, the higher damping encountered during test deployment resulted in a faster decay.

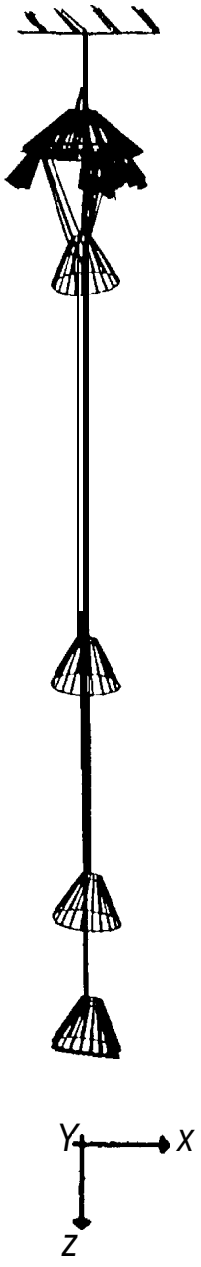

Figure 8. Animation for LSD Test 1

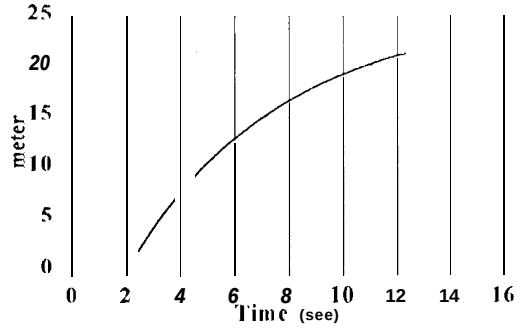

Figure 9. 1 ander CG vs. Time (1 ,SD Test **1)**

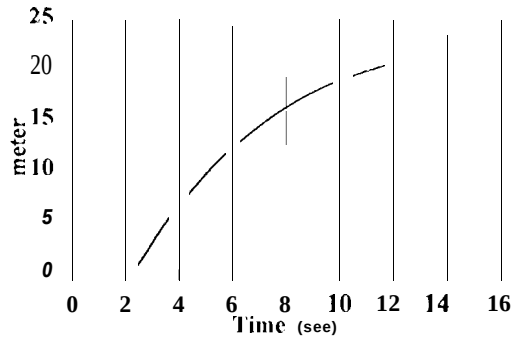

Figure 10. Lander CG vs. Time (TAM)

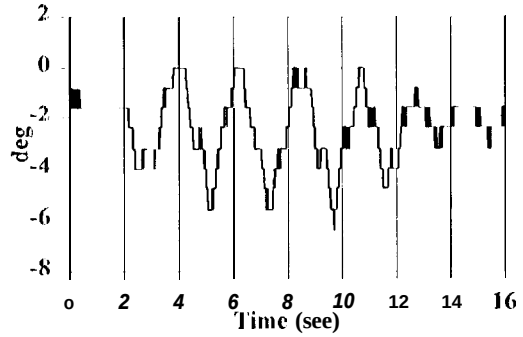

Figure 11. Backshell Rotation about Y Axis (1 ,SD Test 1)

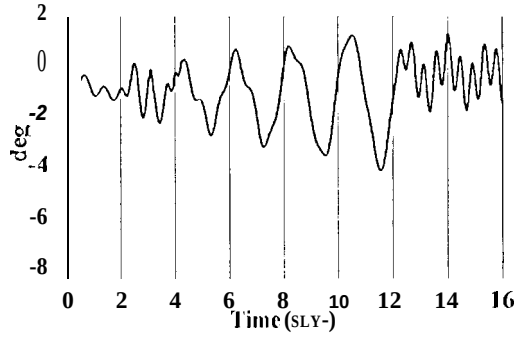

Figure 12. Backshell Rotation about Y Axis (l'AM)

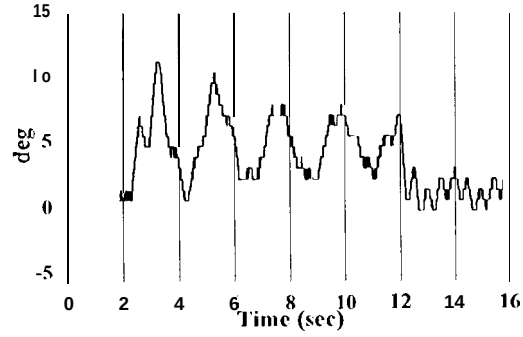

Figure 13. Backshell Rotation about X Axis (1 ,s1) Test 1)

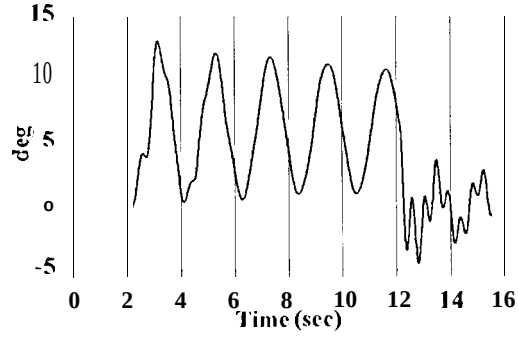

Figure **14.** Backshell Rotation about X Axis ('l'AM)

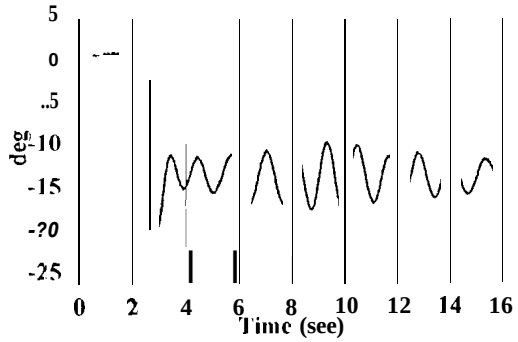

Figure 15. Lander Rotation about X Axis (1 .SDTest 1)

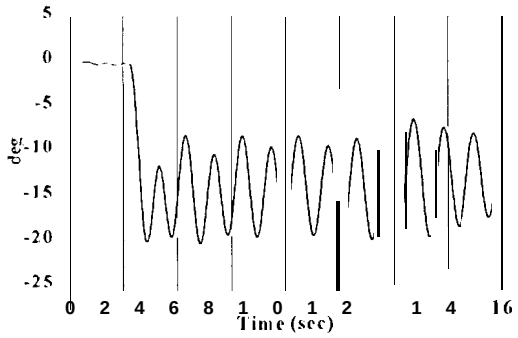

Figure 16. Lander Rotation about X Axis ('1AM)

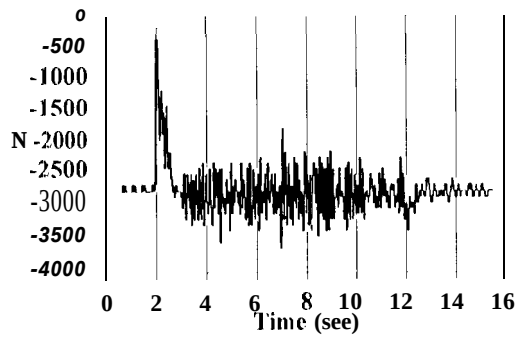

Figure 17. Force in Single Riser (1 .SDTest 1)

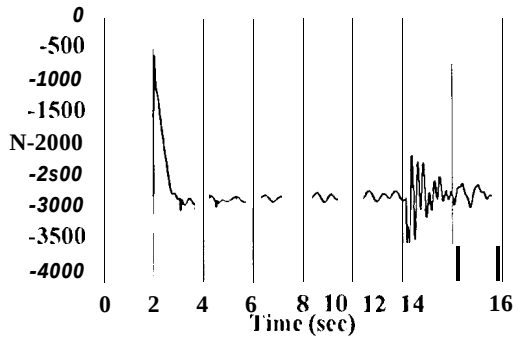

Figure 18. Force in Single Riser (TAM)

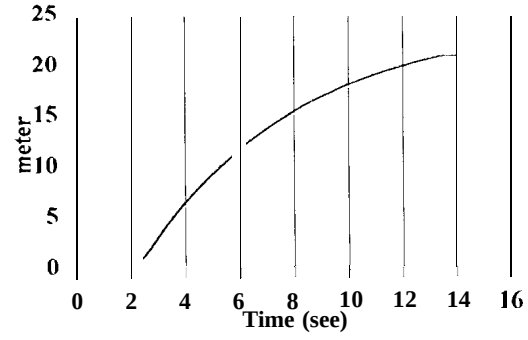

Figure 19. Lander CG vs. Time (1,s1)'1'CS12)

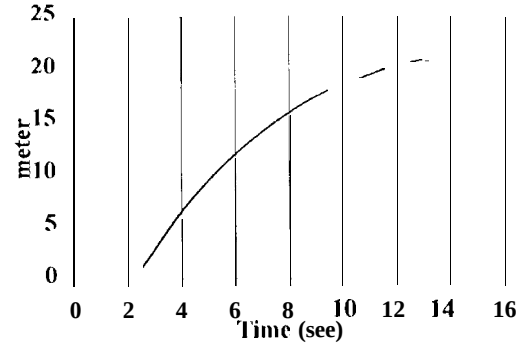

Figure 20. Lander CG vs. Time (l'AM)

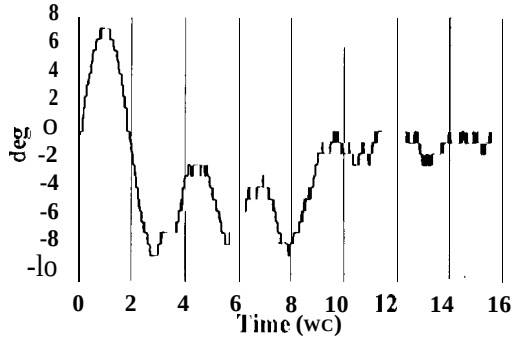

Figure 21. Backshell Rotation about Y Axis (LSD Test 2)

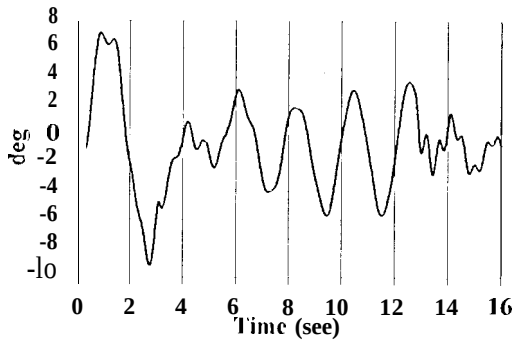

Figure 22. Backshell Rotation about Y Axis ('1AM)

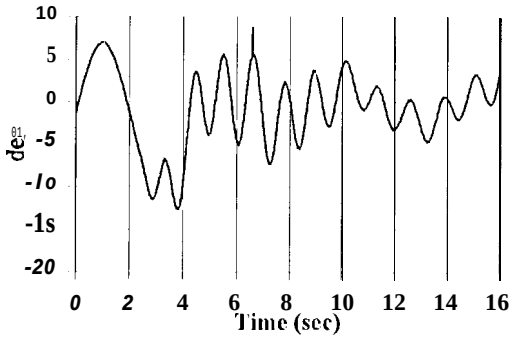

Figure 23. Lander Rotation about Y Axis (1,s1)'1'CS12)

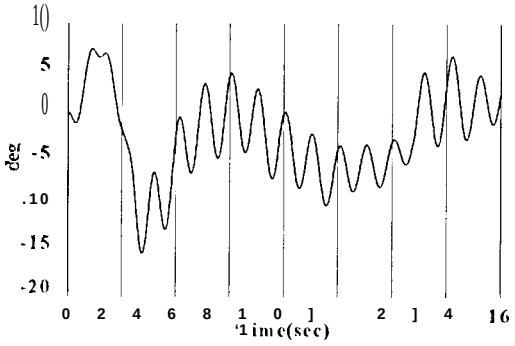

Figure 24. Lander Rotation about Y Axis (TAM)

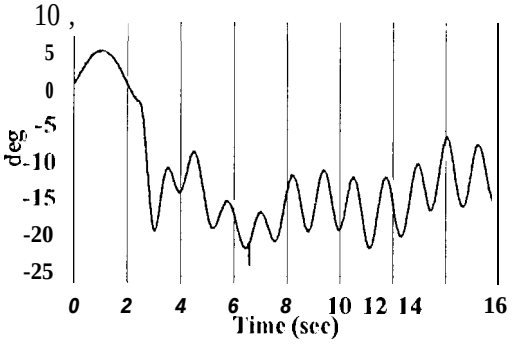

Figure 25. Lander Rotation about X Axis (1 .SD Test 2)

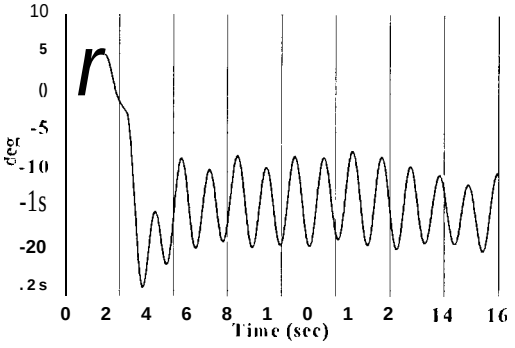

Figure 26. Lander Rotation about X Axis (TAM)

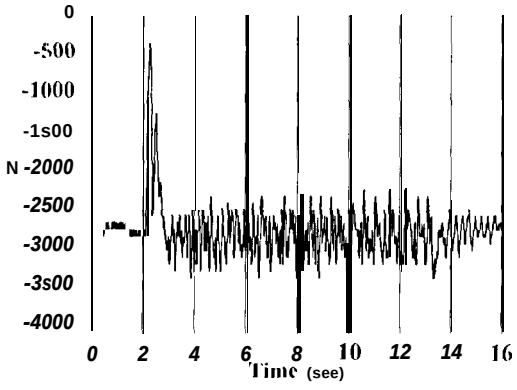

Figure 27. Force in Single Riser (1 .SD Test 2)

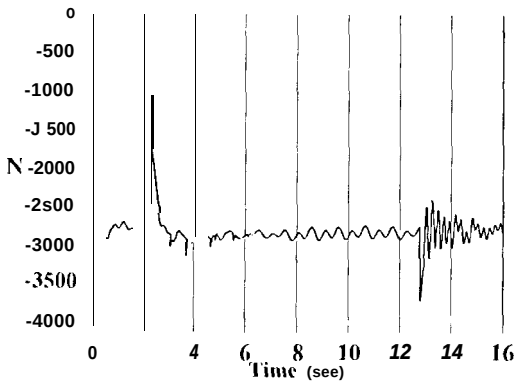

Figure 28. Force in Single Riser (TAM)

The force in the single riser (cable connecting backshell to cci ling) from test and '1 'AM is shown in Figures 17 and 18 respectively.

The analysis predicted the initial force quite accurately although the snatch force al the end of deployment was over-predicted. The reason for this over-prediction may be explained by the higher energy dissipation during test deployment. The actual clamping mechanism included the breaking of stitches connecting the bridle to the petal and was more complex than the viscous model assumed in the 'l'AM.

Correlation for LSD Test 2

Figures 19 and 20 show respectively the vertical displacement of the lander e.g. vs. time from test and TAM. The analysis under-predicts the time of lander deployment by approximately 4°/0.

'1 he backshell rotation about the Y axis from test and TAM is shown in Figures 21 anti 22 respect ivel y. Very good amplitude correlat ion is obtained for the first cycle (initial pendulum swing). 11 owever, the test hardware exhibited greater energy dissipation and the oscillatory amp] it udes arc general l y smaller compared to the analysis, particularly for the later stage of deployment.

Figur es 23 and 24 show respectivel y the lander rotation about the Y axis from test anti TAM. Excel lent agreement is obtained for the oscillatory amplitudes and their variation with time even though the frequency of the response is somewhat over-predi ctcd by the analysis.

The lander rotation about the X axis from test and TAM is shown respectively in Figures 25 and 26. The analysis accurately predicts the initial pendulum motion, but over-predicts both the amplitude and frequency of the response during, deplo yment.

The force in the single riser (cable connecting backshell to ceiling) from test and analysis is shown Figures 27 and 28 respectively. As for 1 .SD Test 1, the analysis predicts the initial force quite accurately although the snatch force at the end of deployment was over-predicted.

6. CONCI USIONS

As described in sections 3 and 5, in general very good agreement between the analytical predictions and test results was achieved by model correlation. As a result, the dynamic model used in the Mars Pathfinder EDI, simulation was successfully validated.

The test verified model will be used to develop a dynamic model for the final end-to-end Mars Pathfinder EDI, simulation. The simulation results will be reviewed to assess the Mars Pathfinder EDI, system performance.

ACKNOWLEDGMENT

The support provided by Mars Pathfinder EDL management team (Brian K. Muirhead, Robert M. Manning, Sam W. Thurman) is gratefully acknowledged.

The work described herein was conducted by Jet Propulsion Laboratory, California Institute of Technology, under contract with National Aeronautics and Space Administration.

REFERENCES

[1] "Mars Pathfinder Project Flight System Requirements and Verification, PF-300-2.0, Rev. A," JPL D-10903, August 1994, Jet Propulsion Laboratory, California Institute of Technology, Pasadena, California.

[2] K. Smith, C-Y. Peng, and A, Behboud, "Multibody Dynamic Simulation of Mars Pathfinder Entry Descent and Landing," JPL D-13298, April 1, 1995, Jet Propulsion Laboratory, [California Institute of Technology, Pasadena, California.

[3] "ADAMS/Solver Reference Manual (V8.0), " Nov. 1994, Mechanical Dynamics, Inc., Ann Arbor, Michigan.

[4] V.N. Sohoni & J. Whitesell, "Automatic Linearization of Constrained Dynamical Systems," ASME J. of Mechanisms, Transmissions & Automation in Design, Sep. 1986, Vol. 108, NO. 3.

Dr.Chia-Yen Peng is a Member of Technical Staff in the Spacecraft Structures and Dynamics Group at the Jet Propulsion Laboratory. His responsibilities are in the areas of Loads and Dynamics for all JPL flight projects. He has worked in the areas of structural dynamics, modal testing and stress analysis in the acrospace and computer industries for 16 years, Dr. Peng received his M. S. and Ph.D. degrees in Applied Mechanics from California Institute of Technology, Pasadena, (California, USA.

Dr. Sai K. Tsang is a Member of Technical Staff in the Spacecraft Structures and Dynamics Group at the Jet Propulsion Laboratory where he has been involved in the numerical simulation and testing of spacecraft systems and subsystems. Prior to joining JPL, he had worked in the areas of structural dynamics anti stress analysis in the aircraft, nuclear anti offshore industries for 15 years. Dr. Tsang received his M.S. and Ph.D. from Imperial College, University of London, UK.

Dr. Kenneth Smith received his Ph.D. from Caltech in 1985, and took a position at the Jet Propulsion Laboratory. While at JPL, he was responsible for loads anti dynamics for all JPL spacecraft programs. In 1996 he joined the staff at SDRC, where he continues to be involved in testing and analysis of a variety of structures.

Dara Sabahi BS 1981 in Civil Engineering from University of California, Los Angeles; Employed by JPL since 1989; Stress analyst for DFM, LPE and SIR-C projects; Chief engineer for SIR-C Antenna Mechanical System; Mechanical System Lead for Mars Pathfinder EDL Subsystem; PEM for Champollion mechanical system,

Kendra Short BSE 1989 in Aerospace Engineering from Princeton University; MSE 1992 in Aeronautics & Astronautics from Stanford University; Joined JPL in 1989; Led advanced concepts studies in Spacecraft Systems Engineering, 89-91; System level requirements & test plans for Mars Pathfinder in Spacecraft Systems Engineering, 92-94; Designed, fabricated, assembled, anti tested Cassini/Mars Pathfinder flight hardware in Spacecraft Mechanical Systems, 94-96.